3

A Multiobjective Evolutionary Algorithm for Hyperspectral Image Watermarking

D. Sal and M. Graña*

Grupo Inteligencia Computacional, UPV/EHU,
Apdo. 649, 20080 San Sebastian, Spain
manuel.grana@ehu.es

Summary. With the increasing availability of internet access to remote sensing imagery, the concern with image authentication and ownership issues is growing in the remote sensing community. Watermarking techniques help to solve the problems raised by this issue. In this paper we elaborate on the proposition of an optimal placement of the watermark image in a hyperspectral image. We propose an evolutionary algorithm for the digital semi-fragile watermaking of hyperspectral images based on the manipulation of the image discrete cosine transform (DCT) computed for each band in the image. The algorithm searches for the optimal localization in the support of an image's DCT to place the mark image. The problem is stated as a multi-objective optimization problem (MOP), that involves the simultaneous minimization of distortion and robustness criteria. We propose appropriate fitness functions that implement these conflicting criteria, and that can be efficiently evaluated. The application of an evolutionary algorithm (MOGA) to the optimal watermarking hyperspectral images is presented. Given an appropriate initialization, the algorithm can perform the search for the optimal mark placement in the order of minutes, approaching real time application restrictions.

3.1 Introduction

The hyperspectral sensor performs a fine sampling of the surface radiance in the visible and near infrared wavelength spectrum. Therefore each image pixel may be interpreted as a high dimensional vector. We are interested in the watermarking of hyperspectral images because all the new remote sensor are designed to be hyperspectral. The fact that Internet is is becoming the primary mean of communication and transport of these images, may raise authentication and ownership issues in the near future.

Watermarking is a technique for image authorship and content protection [21, 1, 15, 16, 20, 22, 13, 23]. Semi-fragile watermarking [12, 24] tries to ensure the image integrity, by means of an embedded watermark which can be recovered without modification if the image has not been manipulated. However, it is desirable that the watermark recovery is robust to operations like filtering, smoothing and lossy compression [19] which are very common while distributing

* The Spanish Ministerio de Educacion y Ciencia supports this work through grant DPI2006-15346-C03-03 and VIMS-2003-20088-c04-04.

M. Graña and R.J. Duro (Eds.): Comput. Intel. for Remote Sensing, SCI 133, pp. 63–78, 2008.
springerlink.com

images through communication networks. For instance, the JPEG lossy compression first standard deletes the image discrete cosine transform (DCT) high frequency coefficients. The JPEG 2000 standard works on the image discrete wavelet transform (DWT) coefficients, also removing high frequency ones as needed to attain the desired compression ratio. Embedding the watermark image in the image transform coefficients is the usual and most convenient approach when trying to obtain perceptually invisible watermarks. We have focused on the DCT transform for several reasons. First it is a real valued transform, so we do not need to deal with complex numbers. Second, the transform domain is continuously evolving from low to high spatial frequencies, unlike DWT which has a complex hierarchical structure in the transform domain. The definition of the fitness functions below benefits from this domain continuity. It is possible to assume some conclusions about the watermark robustness dependence on its placement. Besides being robust, we want the watermarked image must be as perceptually indistinguishable from the original one as possible, that is, the watermarking process must introduce the minimum possible visual distortion in the image.

These two requirements (robustness against filtering and minimal distortion) are the contradicting objectives of our work. The trivial watermarking approach consists in the addition or substitution of the watermark image over the high frequency image transform coefficients. That way, the distortion is perceptually minimal, because the watermark is embedded in the noisy components of the image. However, this approach is not robust against smoothing and lossy compression. The robustness can be enhanced placing the watermark in other regions of the image transform, at the cost of increased distortion. Combined optimization of the distortion and the robustness can be stated as a multi-objective optimization.

Multi-objective optimization problems (MOP) are characterized by a vector objective function. As there is no total order defined in vector spaces, the desired solution does not correspond to a single point or collection of points in the solution space with global optimal objective function value. We must consider the so-called Pareto front which is the set of non-dominated solutions. A non-dominated solution is one that is not improved in all and every one of the vector objective function components by any other solution [6]. In the problem of searching for an optimal placement of the watermark image, the trade-off between robustness and image fidelity is represented by the Pareto front discovered by the algorithm. We define an evolutive strategy that tries to provide a sample of the Pareto front preserving as much as possible the diversity of the solutions. The stated problem is not trivial and shows the combinatorial explosion of the search space: the number of possible solutions is the number of combinations of the image pixel positions over the size of the image mark to be placed.

Section 3.2 provides a review of related previous works found in the literature. Section 3.3 will review multi-objective optimization basics. Section 3.4 introduces the problem notation. Section 3.5 describes the proposed algorithm. Section 3.6

presents some empirical results and section 3.7 gives our conclusions and further work discussion.

3.2 Related Works

The growing number of papers devoted to watermarking of remote sensing images is a proof of the growing concern of this community with authentication and copyright issues. Some of the authors deal with conventional (grayscale) images [8, 5, 14], others with multispectral images (LANDSAT) [3, 4] and some of them with hyperspectral images [10, 17, 9, 18]. In [8] the watermark is applied on the coefficients of the image Hadamard transform. In [10] it is applied to a PCA dimensional reduction of the image wavelet transform coefficients. A near lossless watermarking schema is proposed in [3]. There the effect of watermarking on image classification is the measure of watermarked image quality, while in [4] the watermark placement is decided to minimize the effect on the classification of the image. In [18] two watermarking algorithms are proposed aimed to minimize the effect on target detection. The combination of watermarking and near lossless compression is reported in [5]. The exploration of semi-fragile watermarking based on the wavelet transform is reported in [14]. The watermarking of hyperspectral images performed on the redundant discrete wavelet transform of the pixel spectral signatures is proposed in [17]. The approach in [9] involves 3D wavelet transform and the watermark strength is controlled by perceptive experiments. Our approach allows for greater quantities of information to hide, and provides an variable placement to minimize the effect of the watermark measured by a correlation measure.

3.3 Multi-objective Optimization Problem

Osyczka defined the Multiobjective Optimization Problem (MOP) as "the problem of finding a vector of decision variables which satisfies constraints and optimizes a vector function whose elements represent the objective functions. These functions form a mathematical description of performance criteria which are usually in conflict with each other. Hence, the term *optimize* means finding such a solution which would give the values of all the objective functions acceptable to the decision maker"[2, 6].

The general MOP tries to find the vector $\mathbf{x}^* = [x_1^*, x_2^*, ..., x_n^*]^T$ which will satisfy m inequality constraints $g_i(\mathbf{x}) \geq 0, i = 1, 2, ..., m$, p equality constraints $h_i(\mathbf{x}) = 0, i = 1, 2, ..., p$ and will optimize the vector function $\mathbf{f}(\mathbf{x}) = [f_1(\mathbf{x}), f_2(\mathbf{x}), ..., f_k(\mathbf{x})]^T$.

A vector of decision variables $\mathbf{x}^* \in \mathcal{F}$ is Pareto optimal if it does not exist another $\mathbf{x} \in \mathcal{F}$ such that $f_i(\mathbf{x}) \leq f_i(\mathbf{x}^*)$ for all $i = 1, .., k$ and $f_j(\mathbf{x}) < f_j(\mathbf{x}^*)$ for at least one j. Here $\mathcal{F}$ denotes the region of feasible solutions that meet the inequality constraints. Each solution that carries this property, is called non-dominated solution, and the set of non-dominated solutions is called Pareto

optimal set. The plot of the objective functions whose non-dominated vectors are in the Pareto optimal set is called the Pareto front.

A vector $\mathbf{u} = (u_1, ..., u_n)$ is said to dominate $\mathbf{v} = (v_1, ..., v_n)$ (denoted as $\mathbf{u} \preceq \mathbf{v}$) if and only if $\forall i \in \{1..k\}, u_i \leq v_i \wedge \exists i \in \{1, ..., k\} : u_i < v_i$.

For a given MOP $\mathbf{f}(x)$, the Pareto optimal set $\mathcal{P}^*$ is defined as: $\mathcal{P}^* := \{x \in \mathcal{F} \mid \neg\exists x' \in \mathcal{F} : \mathbf{f}(x') \preceq \mathbf{f}(x)\}$, and the Pareto front ($\mathcal{PF}^*$) is defined as: $\mathcal{PF}^* := \{\mathbf{u} = \mathbf{f} = (f_1(x), ..., f_k(x)) \mid x \in P^*\}$.

3.4 Watermarking Problem and Algorithm Notation

We have an hyperspectral image X of size m_x x n_x x *nbands* that we want to protect. To do that, we use a mark image W of size m_w x n_w. The DCT of the image and the mark image are denoted X_t and W_t respectively. X_t is obtained by applying the bi-dimensional DCT to each band. Watermarking is performed by adding the DCT watermark image coefficients in W_t to selected DCT image coefficients in X_t. Given two coordinates k, l of the W domain, $1 \leq k \leq m_w$, $1 \leq l \leq n_w$, we denote $x(k,l)$, $y(k,l)$, $z(k,l)$ the coordinates of the X_t domain where the coefficient $W_t(k,l)$ is added in order to embed the mark.

The algorithm described below works with a population *Pop* of N_p individuals which are solutions to the problem. We denote O the offspring population. Let be P_s, P_m and P_c the selection, mutation and crossover probabilities, respectively.

To avoid a possible confusion between the solution vector ($\mathbf{x}$) and the original image (X), we will denote the first one as $\mathbf{s}^*$. So, the algorithm will try to find the vector $\mathbf{s}^*$ optimizing $\mathbf{f}(\mathbf{s}) = [f_1(\mathbf{s}), f_2(\mathbf{s})]$ where f_1 is the robustness fitness function and f_2 is the distortion fitness function. The algorithm returns a sampling of the Pareto optimal set $\mathcal{P}^*$ of size between 1 and N_p. The user will be able to select the solution which is better adapted to his necessities from the plotted Pareto front $\mathcal{PF}^*$.

A solution $\mathbf{s}^*$ is represented as an m_w x n_w matrix in which every position $\mathbf{s}^*(k,l)$ of the W_t domain takes three positive values: $x(k,l)$, $y(k,l)$ and $z(k,l)$. Actually, our mark is a small image or logo. The embedded information is the logo's DCT. So, the corruption of the recovered mark is detected by visual inspection, and can be measured by correlation with the original mark.

3.5 Algorithm

In this section we will start introducing the fitness functions that model the robustness and distortion of the solutions. Next we define the operators employed. The section ends with the global definition of the algorithm.

3.5.1 Multi-Objective Fitness

The fitness functions f_1 and f_2 measure the robustness and distortion of the watermark placement represented by an individual solution, respectively. Together, they compose the vector objective function ($\mathbf{f}$) to be optimized.

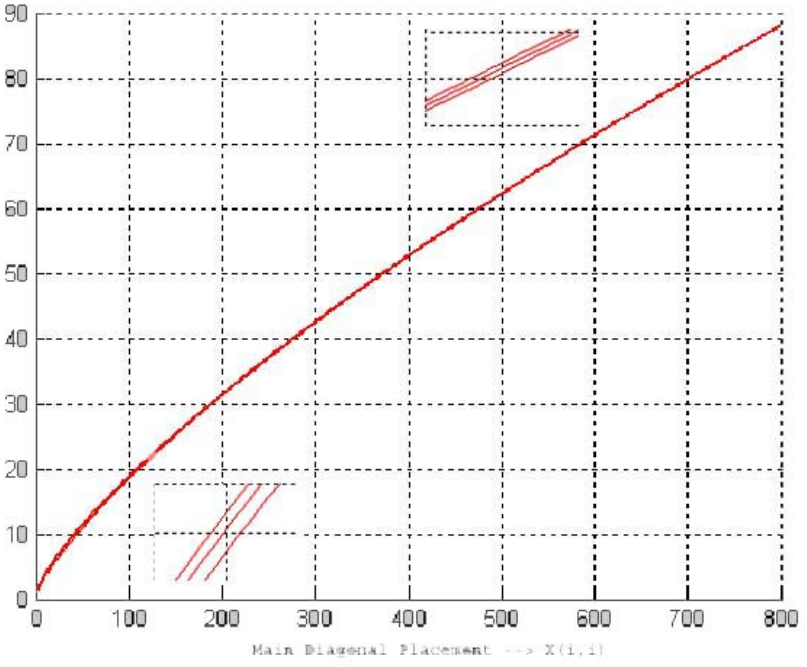

Fig. 3.1. Evolution of f_1, for $F = 4$ and $d = 3$. Insets show zooming the function in specific domains.

Robustness fitness function f_1

Watermark Robustness refers to the ability to recover the watermark image even after the watermarked image has been manipulated. We focus in obtaining robustness against lossy compression and smoothing of the watermarked image. Both transformations affect the high and preserve the low frequency image transform coefficients. Therefore the closer to the transform space origin the mark is located, the higher the robustness of the mark. As we are embedding the watermark image DCT, we note also that most of the watermark image information will be in its low frequency coefficients so.Therefore, they must have priority to be embedded in the positions that are nearer to the low frequencies of X_t. All these requirements are expressed in equations (3.1) and (3.2). Our robustness fitness function is the sum extended to all the watermark pixels of the α-root of the position norm.

$$f_1 = \sum_{k=i}^{m_w} \sum_{l=1}^{n_w} \sqrt[\alpha]{x(k,l)^2 + y(k,l)^2 + k + l} \tag{3.1}$$

where α is given by:

$$\alpha = F\frac{\sqrt{x(k,l)^2+k}+\sqrt{y(k,l)^2+l}}{x(k,l)+y(k,l)+k+l}+d \tag{3.2}$$

Equation (3.1) is based on the Euclidean distance of the position where a mark DCT coefficient $W_t(k,l)$ is placed to the DCT transform X_t domain origin : $\sqrt{x(k,l)^2+y(k,l)^2}$. The terms $k+l$ inside the root expression model the priority of the watermark image DCT low frequency coefficients to be placed on robust placements. However, this distance has an unsuitable behavior to be taken as a fitness function for minimization. Its value decreases very fast when the pixel of the mark is placed near the X_t low frequencies, but remains almost constant when the mark is placed in the low-medium frequencies. This problem is known as the big plateau problem. To avoid this problem, we try to define a fitness function which shows smooth (bounded) but non-negligible variation over all the domain of solutions. To this end we introduce the α-root, with the root exponent being controlled by equation (3.2). The higher value of the root exponent, the closer to a constant value is obtained (although the function continues to have an exponential behavior). The more important the watermark DCT coefficient, the bigger the root exponent and the lower the fitness function. Equation (3.2) is a line function on the following ratio

$$\alpha = \frac{\sqrt{x(k,l)^2}+\sqrt{y(k,l)^2}}{x(k,l)+y(k,l)}$$

which takes values between zero and one. This ratio is modulated by a factor F and a displacement d. As said before, the fitness function has to be sensible to the relative importance of k,l in the watermark image DCT $W_t(k,l)$ domain. Equation (3.2) also introduces this sensitivity by taking into account the k,l coordinates.

Figure 3.1 shows the behavior of f_1 when three different pixels of W_t are embedded in the main diagonal of X_t. The x axis of this plot represent the position in the main diagonal. The function grows smoothly and steadily without plateau effects towards the high frequency region. The insets show that the behavior of the function depends also of the watermark image DCT coefficient $W_t(k,l)$ placed (bigger the lower frequencies).

The robustness fitness does not depend on the band number, because each band DCT has been computed independently. In summary, this function possesses the following properties:

1. As the position in X_t where $S(k,l)$ is embedded is closer to the low frequency region, the function value decreases smoothly.
2. As the pixel of W_t is more important (nearest to the W_t low frequencies), the value of α increases smoothly, so the fitness function decreases smoothly.

Thus, f_1 must be minimized to maximize the robustness.

Distortion fitness function f_2

The watermarking distortion is the mean square error of the watermarked image relative to the original unmarked image. We compute it as the mean squared

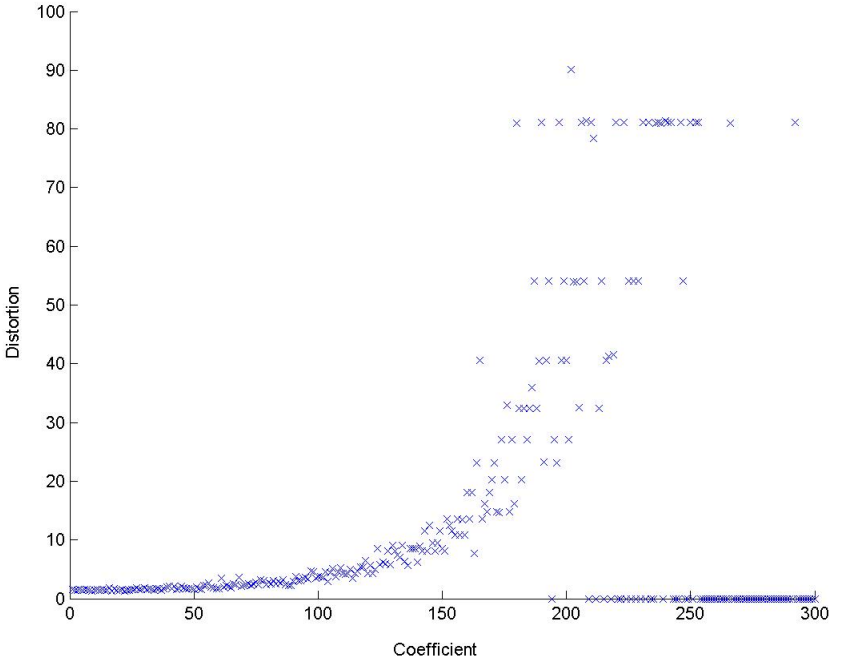

Fig. 3.2. Plot of distortion of the watermarked image versus coefficient magnitude regardless of position

difference between the original image and the inverse of the marked DCT. Minimizing the distortion would be trivially attained by placing the watermark at the higher frequency region of the DCT domain. However, this contradicts our goal of obtaining a maximally robust placement. To avoid the computational cost of the DCT inversion, we propose as the fitness function of the evolutionary algorithm an approximation that follows from the observation that the distortion introduced adding something to a DCT coefficient is proportional to the absolute value of that coefficient. An empirical validation of this assertion is shown in figure 3.2. The computational experiment consisted in repeatedly adding a constant value to single randomly selected coefficients of a test image DCT and computing the distortion of the marked image. There the x axis in the graph is the value of the affected coefficient. The ordinate axis is the distortion value respect the original image. The figure shows that modifications in coefficients with the same value generate different distortion values. This is the effect due to the coefficient placement in the transform domain. In general, the distortion decreases as the the distance to the transform domain origin increases. Nevertheless, it can appreciated that as the affected coefficient magnitude decreases the marked image distortion decreases regardless of the coefficient placement in

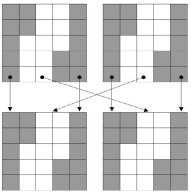

Fig. 3.3. Illustration of the Crossover Operator based on 2 cut points

the transform domain. Thus, the distortion fitness function to be minimized we propose is the following one:

$$f_2 = \sum_{k=i}^{m_w} \sum_{l=1}^{n_w} \mid X_t(x(k,l), y(k,l), z(k,l)) \mid \tag{3.3}$$

3.5.2 Evolutionary Operators

Selection Operator: This operator generates O from P. The populations has previously been ordered according to its range and distance between solutions as proposed in [7]. The selection is realized by random selection of the individuals, giving more probability to the ones at the beginning of the sorted list.

Crossover operator: This operator is applied with probability P_c and is used to recombine each couple of individuals and obtain a new one. Two points from the solution matrix are randomly selected as cut points, and the individuals are recombined as in conventional crossing operators. This operator is illustrated in 3.3.

Mutation operator: Every element of an individual solution $\mathbf{s}$ undergoes a mutation with probability P_m. The mutation of an element consists of displacing it to a position belonging to its 24-Neighborhood in the 3D DCT domain grid: given a pixel $W_t(k,l)$ located in the position $x(k,l), y(k,l), z(k,l)$ of X_t, the new placement of $\mathbf{s}(k,l) \in \{X_t(x(k,l) \pm 1, y(k,l) \pm 1, z(k,l) \pm 1)\}$. The direction of the displacement is randomly chosen. If the selected position is out of the image, or collides with another assignment, a new direction is chosen.

Reduction operator: After applying the selection, crossover and mutation operators we have two populations: parents P and offsprings O. The reduction operator determines the individuals who are going to form the next generation population. Parent and offspring populations are joined in a new one of size $2P_s$. This population is sorted according to the rank of each solution and distance between solutions[7]. This ensures an elitist selection and the diversity of the solutions through the Pareto front. The new population P is composed of the best P_s individuals according to this sorting.

3.5.3 Algorithm

The first step of the GA is the generation of an initial population P and the evaluation of each individual's fitness. The rank and distance of each individual is calculated [7] and is computed to sort P. Once done this, the genetic iteration begins: An offspring population O is calculated by means of the selection, crossover, and mutation operators. The new individuals are evaluated before joining them to the population P. Finally, after computing the reduction operator over the new rank and distance of each individual, we obtain the population P for the next iteration.

Since the GA works with many non-dominated solutions, the stopping criterion compares the actual population with the best generation, individual to individual, by means of the *crowded_comparison*() [7]. If no individual, or a number of individuals below a threshold, improves the best solution in n consecutive iterations, the process is finished. A pseudo-code for de GA is shown in figure 3.4.

```
Pob = Generate_Initial_Population();
Fitness_Function_Evaluation(Pob);
Range=fast_non_dominated_sort(Pob);
Distance=crowding_distance_assignment(Pob);
Stop = false;
While Stop == false
    Couples = Selection_Operator(Pob);
    Of = Merge_Operator(Couples);
    Of = Mutation_Operator(Of);
    Fitness_Function_Evaluation(Of);
    Pob = Join(Pob,Of);
    Range = fast_non_dominated_sort(Pob);
    Distance = crowding_distance_assignment(Pob);
    Pob = ordering(Pob, Range, Distance);
    Pob = Reduction_Operator(Pob);
    Evaluate_Stop_Criterium():
end while;
plot(Pareto-Front);
```

Fig. 3.4. Pseudo-code for the proposed GA

The Pareto front is formed by the set of solutions with rank = 1. Once finished the process and chosen a solution, the mark is embedded adding its coefficients to the coefficients of X_t according to the corresponding value of $\mathbf{s}^*$. Before the coefficients are added, they are multiplied by a small value.

3.6 Results

This results section contains an example application to a conventional gray level scale, that could correspond to a panchromatic remote sensing image. We show

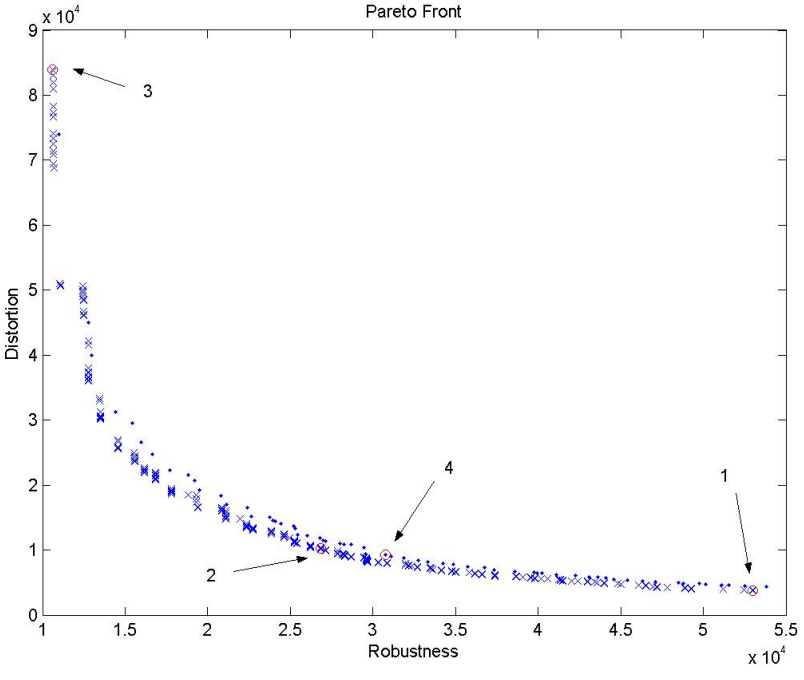

Fig. 3.5. Pareto fronts found by GA and local search, identified by 'x' and '.' respectively

Fig. 3.6. From left to right: Original Image; Images watermarked using the placement denoted in figure 3.5 as solution 3, as solution 2 and as solution 1

that proposed algorithm finds robust and low distortion watermark placements, therefore the proposed fitness functions can be assumed to model appropriately the desired watermark properties. Then we extend the results to a well known benchmark hyperspectral image.

3.6.1 Results on a Conventional Gray Level Image

The results presented in this section concern the application of the algorithm over an image of size 400 x 500. The image DCT X_t has been divided in 676

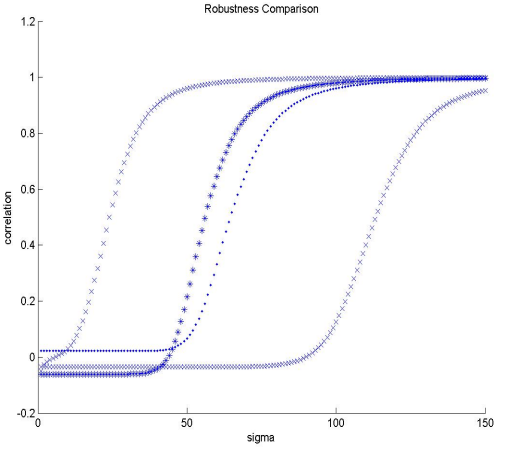

Fig. 3.7. Robustness measured as the correlation coefficient of the recovered image mark versus the radius of the gaussian smoothing filter. Each curve corresponds to a placement solution identified in in figure 3.5. Solutions 1 and 3 are represented by 'x'. Solution 2 by '*' and Solution 4 by '.'.

Fig. 3.8. Watermark logo: Original and recovered from the image watermarked using placement solution 2 in figure 3.5 after it has been low-pass filtered with *sigma* = 50, 60, 70, 80, 90, 100

overlapping and regular image blocks of size 100 x 100. The initial population is formed by 672 individuals each one placed randomly in a different quadrant. As the watermark image we have used an image of size 32 x 32. The GA was executed with $P_s = 20, P_m = 0.05$ and $P_c = 0.9$. We set the robustness fitness f_1 parameters to $F = 4$ and $d = 3$.

For comparison purposes the problem has been solved by means of a random local search starting from the same random initial conditions. This local search consist only of proposing a new placement by a random perturbation computed like the mutations above. This new placement is accepted if it does improve the current solution. The local search stops when a number of proposed placements are rejected, assuming that the algorithm is stuck in a local optimum. Figure 3.5 shows the Pareto-Front found with both algorithms. The GA has found 329 non-dominated solutions while the local search only found 62. Besides the GA solutions dominate all the solutions found by the local search.

We have pointed out and numbered in figure 3.5 some very specific solutions. The solution denoted as 1 corresponds to the solution with the lowest fitness

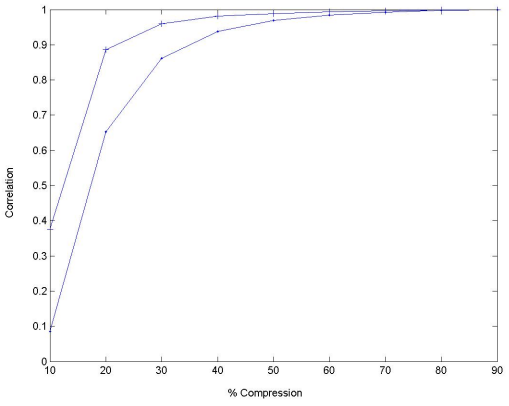

Fig. 3.9. Robustness of watermark placement solutions 2 ('.') and 4 ('+') in in figure 3.5 to JPEG compression. Correlation of the recovered mark image versus compression quality.

distortion value, regardless of the robustness fitness value (which is very high). The solution signaled as 3 corresponds to the solution with lowest robustness fitness, regardless of the fitness distortion value (again very high). These solutions correspond to optima of the objective criteria taken in isolation. We consider also compromise solutions 2 and 4 that correspond to the best robustness for a set upper limit of the distortion, taken from the Pareto fronts found by the GA (solution 2) and the local search (solution 4). Figure 3.6 shows the experimental image (left) and the visual results of GA generated watermark placement solution. The distortion is almost no perceptible, but for the image corresponding to solution 3 in figure 3.5.

To asses the robustness of the watermark placements found, we compute the correlation coefficient between the original watermark and the watermark recovered from the watermarked image after it has been smoothed by a low-pass gaussian filter applied in the Fourier transform domain. The figure 3.7 plots the correlation coefficients versus the increasing filter radius *sigma* for each of the selected watermark placement solutions selected in figure 3.5 . This plot shows that the watermark placement solution 2 obtains a good correlation coefficient for lower values of *sigma* than solution 1 (note that in figure 3.6 there are no perceptual differences between both images). That means that the GA found a solution that is much more robust than the one with minimal distortion while preserving much of the distortion quality. It can be appreciated also in figure 3.7 that the robustness is higher in the solution 2 (GA) than in the solution 4 (Local Search) . Figure 3.8 shows the visual results of the recuperation of the mark image after smoothing the image watermarked using the placement from solution 2.

The second class of attacks we are considering are the lossy compression. We apply the standard jpeg compression with increasing quality factor to the watermarked image, and we recover the watermark image from the decompressed

image. Figure 3.9 shows the correlation of the recovered mark image relative to the original mark image versus compression quality, for the local search and GA watermark placement solutions identified as 4 and 2 in in figure 3.5 . It can be appreciated that the GA solution recovers much better than the local search solution from strong lossy compression.

3.6.2 Results on an Hyperspectral Image

The results presented in this section concern the application of the algorithm over the well known AVIRIS Indian Pines hyperspectral image of size 145 x 145 x 220. The image DCT transform X_t has been divided in 1452 overlapping quadrants of size 45 x 45 x 110. The initial population is formed by 1452 individuals each one placed randomly in a different quadrant. The watermark is an image of size

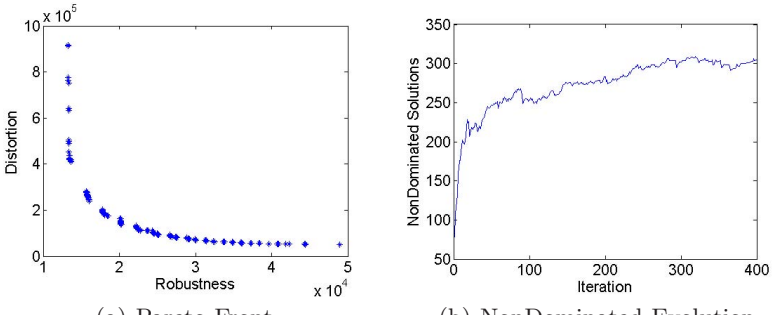

(a) Pareto-Front (b) NonDominated Evolution

Fig. 3.10. a) Pareto front found by GA. b)Evolution of the number of non-dominated solution found by the GA.

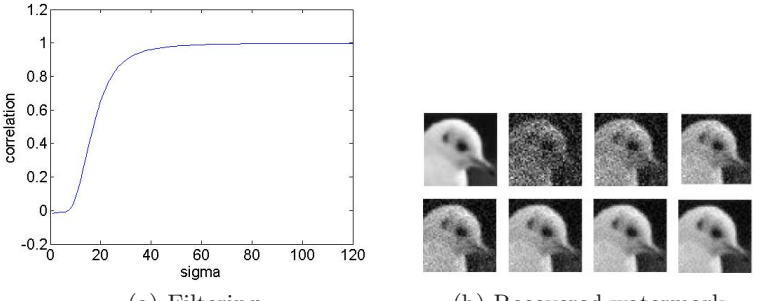

(a) Filtering (b) Recovered watermark

Fig. 3.11. a) Robustness level by means of the correlation coefficient of the recovered image mark versus the radius of the smoothing convolution kernel. b) Original watermark and watermark recovered after low pass filtering with sigma = 10, 20, 30, 40, 50, 60 and 70 respectively.

50 x 50. The GA was executed with $P_s = 20, P_m = 0.05$ and $P_c = 0.9$. We fit the response of the robustness fitness f_1 with $F = 4$ and $d = 3$.

Figure 10(a) shows the Pareto front consisting of 303 non-dominated solutions, found by the algorithm, following the evolution shown in Figure 10(b). Figure 11(a) plots the correlation coefficient between the original watermark and the watermark recovered after each band image of the watermarked image has been smoothed by a low-pass gaussian filter with increasing filter radius applied in the Fourier transform domain. Figure 11(b) shows the visual results of the recuperation of the mark image after smoothing the watermarked image.

Studying each pixel spectrum, experts can know which material form the area represented by this pixel. Automated classification systems can be constructed [11] to perform this task. This is the main objective of hyperspectral imaging, so, it is critical that the watermarking process doesn't disturb the spectral content of the pixels. For the noisiest of the solutions shown in Figure 10(a) we computed the correlation of each pixel spectrum with the corresponding one in the original image. The worst value obtained was 0.999. Therefore, this watermarking process is not expected to influence further classification processes.

3.7 Conclusions

We present an evolutionary algorithm to find a watermark's image placement in an hyperspectral image to protect it against undesirable manipulations. It is desirable that the watermark remains recognizable when the image is compressed or low-pass filtered. We state the problem as a multiobjective optimization problem, having two fitness functions to be minimized. The algorithm tries to obtain the Pareto front to find the best trade-off between distortion of the original image in the embedding process and robustness of the mark. The solutions found by the GA provide strong robustness against smoothing manipulations of the image. Because the algorithm works with the entire image DCT, it can be used to hide bigger images or data chunks than other similar approaches. Also it will be more robust than approaches based on small block embedding, experimental verification is on the way to prove this intuition. Furher work must be addressed to the extension of this approach to wavelet transforms of the images.

References

1. Augot, D., Boucqueau, J.M., Delaigle, J.F., Fontaine, C., Goray, E.: Secure delivery of images over open networks. Proceedings of the IEEE 87(7), 1251–1266 (1999)
2. Back, T., Fogel, D.B., Michalewicz, T.: Evolutionary Computation1. Basic Algorithms and Operators. Board Addison-Wesley Publishing Company, Reading (2000)
3. Barni, M., Bartolini, F., Cappellini, V., Magli, E., Olmo, G.: Near-lossless digital watermarking for copyright protection of remote sensing images. In: IGARSS 2002, vol. 3, pp. 1447–1449. IEEE Press, Los Alamitos (2002)

4. Barni, M., Magli, E., Troia, R.: Minimum-impact-on-classifier (mic) watermarking for protection of remote sensing imagery. In: IGARSS 2004, vol. 7, pp. 4436–4439 (2004)
5. Caldelli, R., Macaluso, G., Barni, M., Magli, E.: Joint near-lossless watermarking and compression for the authentication of remote sensing images. In: IGARSS 2004, vol. 1, p. 300 (2004)
6. Coello Coello, C.A., Toscano Pulido, G., Mezura Montes, E.: Current and future research trends in evolutionary multiobjective optimization. In: Graña, M., Duro, R., d'Anjou, A., Wang, P.P. (eds.) Information Processing with Evolutionary Algorithms, pp. 213–232. Springer, New York (2004)
7. Deb, K., Pratap, A., Agarwal, S., Meyarivan, T.: A fast and elitist muliobjective genetic algorithm: Nsga-ii. IEEE transactions on evolutionary computation 6(2), 182–197 (2002)
8. Ho, A.T.S., Jun, S., Hie, T.S., Kot, A.C.: Digital image-in-image watermarking for copyright protection of satellite images using the fast hadamard transform. In: IGARSS 2002, vol. 6, pp. 3311–3313 (2002)
9. Kaarna, A., Parkkinen, J.: Multiwavelets in watermarking spectral images. In: IGARSS 2004, vol. 5, pp. 3225–3228 (2004)
10. Kaarna, A., Toivanen, P.: Digital watermarking of spectral images in pca/wavelet-transform domain. In: IGARSS 2003, vol. 6, pp. 3564–3567 (2003)
11. Landgrebe, D.A.: Signal Theory Methods in Multispectral Remote Sensing Signal Theory Methods in Multispectral Remote Sensing. Wiley-Interscience, Chichester (2003)
12. Maeno, K., Qibin, S., Shih-Fu, C., Suto, M.: New semi-fragile image authentication watermarking techniques using random bias and nonuniform quantization. Multimedia, IEEE Transactions 8(1), 32–45 (2006)
13. Nikolaidis, A., Pitas, I.: Region-based image watermarking. IEEE Transactions on image processing 10(11), 1726–1740 (2001)
14. Qiming, Q., Wenjun, W., Sijin, C., Dezhi, C., Wei, F.: Research of digital semi-fragile watermarking of remote sensing image based on wavelet analysis. In: IGARSS 2004, vol. 4, pp. 2542–2545 (2004)
15. Schneck, P.B.: Persistent access control to prevent piracy of digital information. Proceedings of the IEEE 87(7), 1239–1250 (1999)
16. Young, K.T., Hyuk, C., Kiryung, L., Taejeong, K.: An asymmetric watermarking system with many embedding watermarks corresponding to one detection watermark. Signal Processing Letters 11(3), 375–377 (2004)
17. Tamhankar, H., Bruce, L.M., Younan, N.: Watermarking of hyperspectral data. In: IGARSS 2003, vol. 6, pp. 3574–3576 (2003)
18. Tamhankar, H., Mathur, A., Bruce, L.M.: Effects of watermarking on feature efficacy in remotely sensed data. In: IGARSS 2004, vol. 1, p. 280 (2004)
19. Tang, X., Pearlman, W.A., Modestino, J.W.: Hyperspectral image compression using three-dimensional wavelet coding. In: Image and Video Communications and Processing 2003, Proceedings of SPIE, vol. 5022, pp. 1037–1047. SPIE Press (2003)
20. Vleeschouwer, C., Delaigle, J.F., Macq, B.: Invisibility and application functionalities on perceptual watermarking- an overview. Proceedings of the IEEE 90(1), 64–77 (2002)
21. Voyatzis, G., Pitas, I.: The use of watermarks in the protection of digital multimedia products. Proceedings of the IEEE 87(7), 1197–1207 (1999)

22. Wolfgang, R.B., Podilchuk, C.I., Delp, E.J.: Perceptual watermarking for digital images and video. Proceedings of the IEEE 87(7), 1108–1126 (1999)
23. Yuan, H., Zhang, X.P.: Multiscale fragile watermarking based on the gaussian mixture model. Image Processing, IEEE Transactions 15(10), 3189–3200 (2006)
24. Zou, Y.Q., Shi, D., Ni, Z., Su, W.: A semi-fragile lossless digital watermarking scheme based on integer wavelet transform. Circuits and Systems for Video Technology, IEEE Transactions 16(10), 1294–1300 (2006)